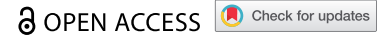


RESEARCH PAPER



## Enterotoxigenic *Bacteroides fragilis* induces the stemness in colorectal cancer via upregulating histone demethylase JMJD2B

Qian-Qian Liu\*, Chun-Min Li\*, Lin-Na Fu\*, Hao-Lian Wang, Juan Tan, Yun-Qian Wang, Dan-Feng Sun, Qin-Yan Gao, Ying-Xuan Chen, and Jing-Yuan Fang

Division of Gastroenterology and Hepatology, Key Laboratory of Gastroenterology and Hepatology, Ministry of Health, State Key Laboratory for Oncogenes and Related Genes, Shanghai Institute of Digestive Disease, Renji Hospital, School of Medicine, Shanghai Jiao Tong University, Shanghai, China

### ABSTRACT

The enrichment of Enterotoxigenic *Bacteroides fragilis* (ETBF) has been identified in CRC patients and associated with worse prognosis. Cancer stem cells (CSCs) play essential roles in CRC development. However, whether ETBF is involved in CSCs regulation is unknown. To clarify the role of ETBF in CSCs properties, we performed extreme limited dilution assays (ELDA) in nude mice injected with ETBF-treated or untreated CRC cells subcutaneously, tumor organoids culture in azoxymethane (AOM) mouse model after gavaging with or without ETBF, and cell sphere formation assay after incubating CRC cell lines with or without ETBF. The results indicated that ETBF increased the stemness of CRC cells *in vivo* and *in vitro*. Furthermore, ETBF enhanced the expression of core stemness transcription factors Nanog homeobox (NANOG) and sex determining region Y-box 2 (SOX2). Histone H3 Lysine 9 trimethylation (H3K9me3) is critical in regulating CSCs properties. As an epigenetic and transcriptional regulator, JmjC-domain containing histone demethylase 2B (JMJD2B) is essential for embryonic stem cell (ESC) transformation and H3K9me3 demethylation. Mechanistically, ETBF infection significantly upregulated JMJD2B levels in CRC cell lines and nude mice xenograft model. JMJD2B epigenetically upregulated NANOG expression via demethylating its promoter H3K9me3, to mediate ETBF-induced stemness of CRC cells. Subsequently, we found that the Toll-like receptor 4 (TLR4) pathway, activated by ETBF, contributed to the enhanced expression of JMJD2B via nuclear transcription factor nuclear factor of activated T cells 5 (NFAT5). Finally, in human CRC samples, the amount of ETBF positively correlated with nuclear NFAT5, JMJD2B, and NANOG expression levels. In summary, ETBF upregulated JMJD2B levels in a TLR4-NFAT5-dependent pathway, and played an important role in stemness regulation, which promoted colorectal carcinogenesis.

### ARTICLE HISTORY

Received 18 February 2020  
Revised 29 May 2020  
Accepted 18 June 2020

### KEYWORDS

Enterotoxigenic *Bacteroides fragilis*; colorectal cancer; stemness; histone demethylase; JMJD2B


## Introduction

Colorectal cancer (CRC) is the third most common cancer worldwide.<sup>1,2</sup> The gut microbiota, along with genetic and other environmental factors, contributes to the carcinogenesis of CRC. Evidence for microbiota involvement in colorectal carcinogenesis can be found in animal models of intestinal carcinogenesis, where both antibiotic-treated conventional and germ-free mice models developed cancer after gavage with fecal samples from patients with CRC. Enterotoxigenic *Bacteroides fragilis* (ETBF) is a human colonic symbiotic anaerobe that is prevalent in up to 50% of the healthy individuals.<sup>3</sup> A link between ETBF and inflammatory bowel disease,<sup>4</sup> as well as CRC, has

been established. Recent clinical data have shown that ETBF is significantly enriched in stool and mucosa samples from patients with CRC compared with those in the healthy controls.<sup>5,6</sup> Moreover, the prevalence of ETBF in CRC tissues is associated with poor prognosis.<sup>3</sup> Researchers have shown that mice implanted with ETBF and *Escherichia coli* are more likely to develop CRC and die.<sup>7</sup> Furthermore, ETBF might promote colorectal carcinogenesis by activating the nuclear factor kappa B (NF- $\kappa$ B) or Wnt signaling pathways,<sup>8,9</sup> increasing polyamine metabolism,<sup>10</sup> inducing DNA damage,<sup>11</sup> and activating Th17 adaptive immunity.<sup>12,13</sup> However, ETBF's possible mechanisms in CRC remain unclear.

**CONTACT** Xuan Chen  [yingxuanchen71@sjtu.edu.cn](mailto:yingxuanchen71@sjtu.edu.cn); Qin-Yan Gao  [gaoqinyan@hotmail.com](mailto:gaoqinyan@hotmail.com)  Division of Gastroenterology and Hepatology, Key Laboratory of Gastroenterology and Hepatology, Ministry of Health, State Key Laboratory for Oncogenes and Related Genes, Renji Hospital, School of Medicine, Shanghai Institute of Digestive Disease, Shanghai Jiao Tong University, Shanghai 200001, China

\*These authors contributed equally to this work. The authors declare no potential conflicts of interest.

 Supplemental data for this article can be accessed [here](#).

© 2020 The Author(s). Published with license by Taylor & Francis Group, LLC.

This is an Open Access article distributed under the terms of the Creative Commons Attribution License (<http://creativecommons.org/licenses/by/4.0/>), which permits unrestricted use, distribution, and reproduction in any medium, provided the original work is properly cited.

Cancer stem cells (CSCs), also called tumor-initiating cells (TICs), are a subset of tumor cells that exhibit self-renewal ability.<sup>14,15</sup> Colorectal CSCs are positively associated with higher recurrence rates.<sup>16,17</sup> CRC with stem cell signatures, such as CD44 positivity, NANOG positivity, or SOX2 positivity, have been associated with resistance to several anticancer drugs, for example, cisplatin, 5-fluorouracil (5-FU), irinotecan, and oxaliplatin.<sup>18–20</sup> Therefore, advancing our understanding of the molecular properties and signaling pathways unique to CSCs is vital to develop a new generation of targeted and effective therapies for CRC. The self-renewal of CSCs results from a complex interplay between gene regulation and the environment. A recent study published in *Science* reported that acidophilic infection can enhance the activity of intestinal stem cells.<sup>21</sup> *Enterococcus faecalis* colonized in the intestinal epithelium of mice promoted the development of CRC by increasing the expression of tumor stem cell markers.<sup>22</sup> Study has also shown that nonpathogenic *E. coli* upregulates the expression of CSC markers, thus engendering tumorigenic stemness in host cells.<sup>23</sup> Thus, bacterial infections might increase the incidence of CRC by stimulating stem cell activity. However, the regulation by ETBF of CSC properties remains largely unknown.

In the present study, we investigated whether ETBF induces stemness during tumorigenesis of CRC and the molecular mechanisms involved. We found that JmjC-domain containing histone demethylase 2B (JMJD2B), which is induced by ETBF in a Toll-like receptor (TLR) 4-nuclear factor of activated T-cells 5 (NFAT5)-dependent manner, plays an important role in the stemness of human CRC cells, which could promote the expression of NANOG by binding and removing the inhibitory H3K9me3 marks on the NANOG promoter region. This study illustrates a new mechanism of promoting the development of CRC mediated by a specific pathogen.

## Results

### ETBF promotes colorectal tumorigenesis *in vivo* and is enriched in CRC patients with advanced TNM stage

It was reported that ETBF-induced inflammatory colitis progressed to colon tumorigenesis in Min mice.<sup>12</sup> To demonstrate the effects of ETBF on

CRC tumorigenicity *in vivo*, we established two different animal models, the AOM-induced sporadic CRC model and the nude mouse xenograft model. In the AOM model, after microbiota depletion using antibiotics (Supplementary Figure S1A), NTBF or ETBF (Supplementary Figure S1B) were introduced to the mice, accompanied by intraperitoneal injection of AOM. We observed that treatment with ETBF significantly increased the number and volume of intestinal tumors in the AOM-injected mice, as compared with the control group and NTBF-gavaged group (Supplementary Figure S1 C, D). A similar role of ETBF was found in the xenograft tumors in nude mice (Supplementary Figure S1E). To identify the clinical significance of ETBF, we performed real-time PCR to quantify the abundance of ETBF in CRC tissue from 56 patients with CRC with different clinicopathological features. According to their ETBF abundance, the patients with CRC were divided into two groups (26 ETBF-low or 30 ETBF-high expression). The correlations between ETBF abundance and clinicopathological factors (age, sex, tumor size, location, TNM stage, and histology) were evaluated and are presented in Table 1. TNM stage III and IV in the ETBF-high group were more frequent than in the ETBF-low group ( $P = .025$ ). Relative ETBF abundance in TNM stage III and IV is higher than that in TNM stage I and II (Supplementary Figure S1 F). Collectively, these results confirmed the pro-tumorigenicity effect of ETBF in CRC, and suggested that ETBF abundance might be positively related with poor prognosis.

### ETBF induces stem cell-like properties *in vitro* and *in vivo*

Recent studies showed that ETBF promoted CRC through affecting proliferation,<sup>9</sup> apoptosis,<sup>24</sup> metabolism,<sup>10</sup> and immunity.<sup>25,26</sup> However, the role of ETBF in CSCs properties is unknown. In order to investigate the effect of ETBF in stem cell-like phenotype regulation in CRC *in vivo*, we performed intestinal organoid culture using individual CRC specimens from AOM-injected mice and extreme limited dilution assays (ELDA<sup>27</sup>) using xenograft tumors in nude mice, respectively. We found that the growth and size of the tumor organoids increased in the ETBF-gavaged group

**Table 1.** Characteristics of CRC patients according to ETBF status.

Clinical characteristics	Patients (N = 56)	The expression of ETBF		P value*
		Low (N = 26)	High (N = 30)	
Gender- no. (%)				.789
Man	30 (53.6)	13 (50)	17 (57)	
Women	26 (46.4)	13 (50)	13 (43)	
Age (mean, y)	67.5	67.61	67.3	.964
Tumor size (mean, cm)	3.78	3.81	3.75	.899
Tumor location				.293
Left colon	26 (46.4)	14 (53.8)	12 (40)	
Right colon	28 (50)	12 (46.2)	16 (53.3)	
Rectum	2 (3.6)	0 (0)	2 (6.7)	
TNM- no. (%)				.025
I-II	32 (57.1)	19 (69.2)	13 (46.7)	
III-IV	24 (42.9)	7 (30.8)	17 (53.3)	
Pathological type				.066
Tubular adenocarcinoma	47 (83.9)	19 (73.1)	28 (93.3)	
Mucinous adenocarcinoma	9 (16.1)	7 (26.9)	2 (6.7)	
Histo-differentiation				.094
Well/moderate	53 (94.6)	23 (88.5)	30 (100)	
Poor differentiation	3 (5.4)	3 (11.5)	0 (0)	

\*: Statistical significance was determined by  $\chi^2$ -test

compared with those of the control, or NTBF-gavaged groups in AOM-injected mice (Figure 1A). In the xenograft model, transplantation of limiting numbers of HCT116 cells into nude mice induced a 2.14-fold increase in the absolute number of TICs in the tumor from ETBF-stimulated mice (1/380202) compared with those from the controls (1/815769) (Figure 1B).

To further evaluate the role of ETBF in regulating stemness *in vitro*, we co-cultured CRC cell lines HCT116 and DLD1 with ETBF, and then analyzed their tumorsphere formation capacity. ETBF significantly increased the number of spheres (diameter  $\geq 100 \mu\text{m}$ ) compared with the Broth control or NTBF group (Figure 1C). NANOG, SOX2, and Octamer-binding transcription factor 4 (OCT4) make up the core transcriptional network responsible for the regulation of stem cell self-renewal and pluripotency.<sup>28,29</sup> Among them, Nanog may be the signaling hub that controls the other core ESC transcription factors.<sup>30,31</sup> In this study, core transcription factors for CSCs, NANOG, SOX2 and OCT4 were compared by real-time PCR and western blotting. We found that NANOG and SOX2 were significantly elevated in the ETBF-infected cells, at both mRNA and protein level, while OCT4 showed no significant change (Figure 1D, E). In line with the above results, real-time PCR and histological staining also revealed that the tumor organoids collected from ETBF-gavaged

C57BL/6 mice and tumors in the ETBF-stimulated nude mice expressed higher levels of NANOG than did in the controls (Figure 1F,G).

Thus, all these data indicated that ETBF increases the stemness of CRC cells *in vitro* and *in vivo*.

### **JMJD2B epigenetically upregulates NANOG expression to mediate ETBF-induced stemness of CRC cells**

The gut microbiota affects host tissue H3 methylation patterns, suggesting a role for the gut microbiota as a driver of chromatin regulation.<sup>32</sup> JMJD2B was identified as an H3K9me3/2 demethylase that activates target gene transcription. To analyze the role of JMJD2B in ETBF-induced stemness in CRC, we first observed JMJD2B expression after ETBF incubation. The results revealed that JMJD2B was significantly upregulated in the ETBF-infected cells (Figure 2A), whereas the protein levels of JMJD2A, JMJD2C, and JMJD2D, the other members of the JMJD2 family, were not induced (Supplementary Figure S2A). Next, we studied whether other CRC-related gut microbiota induced JMJD2B expression. Western blotting showed that the effect of ETBF in upregulating JMJD2B was the most obvious in CRC cells when compared with *E. coli*, *F. nucleatum*, and *C. symbiosum* (Supplementary Figure S2B). Given JMJD2B is a key rate-limiting enzyme that regulates stem cell activity,<sup>33</sup> we further examined whether

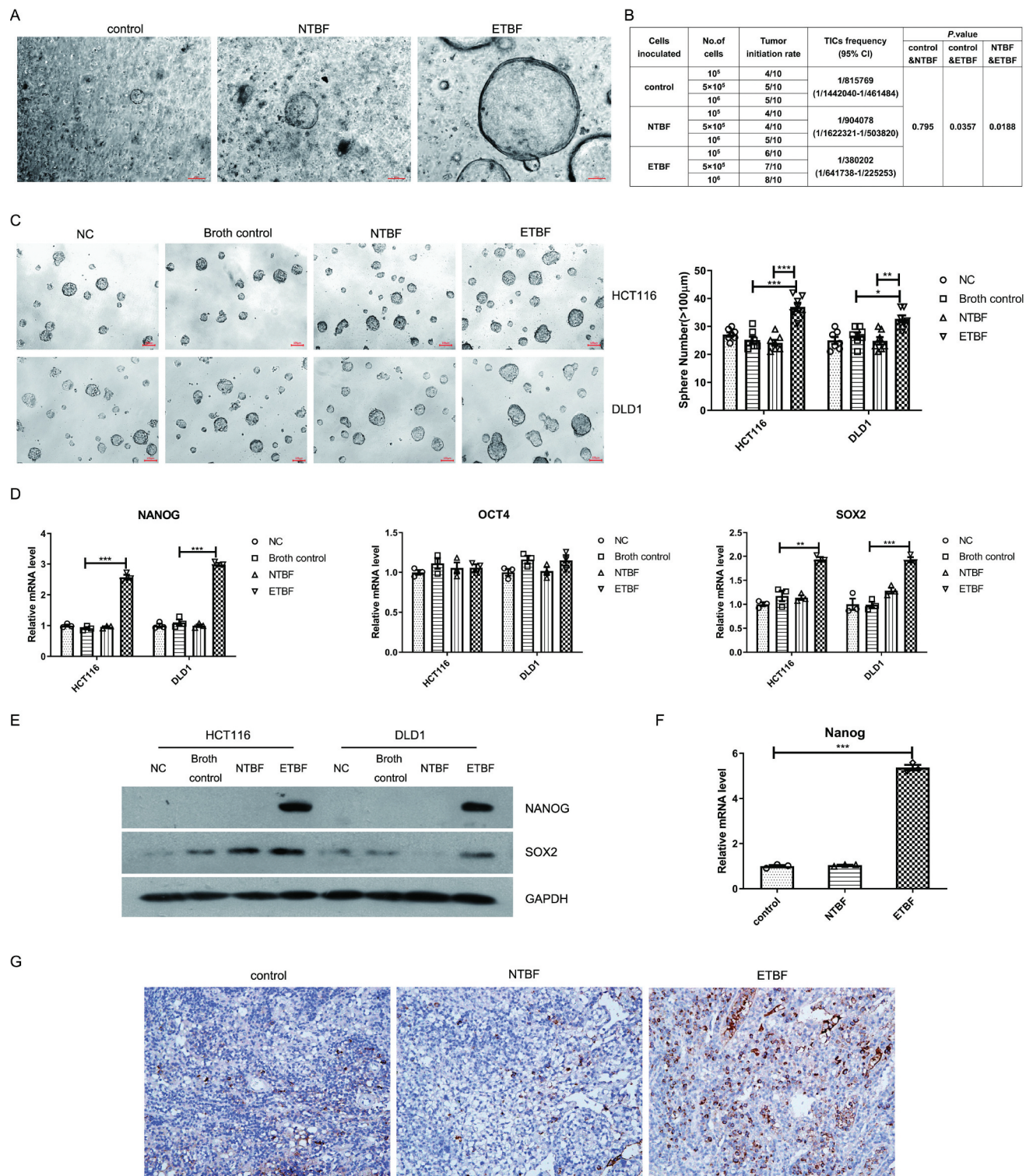


**Figure 1.** ETBF induces stem cell-like properties *in vitro* and *in vivo*. **A**, Representative images of organoids obtained from tumors of NTBF/ETBF-gavaged mice of the AOM model. Circles in graph indicate individual organoid cultures. Scale bar, 100  $\mu$ m. **B**, The extreme limiting dilution analysis (ELDA) to calculate the tumor initiating CSC frequency after transplantation of limiting numbers of HCT116 cells co-cultured with NTBF or ETBF into nude mice. **C**, HCT116 and DLD1 cells (1000 cells/200  $\mu$ L per well) were co-cultured with cell culture medium (NC) or bacteria culture medium (Broth control) as controls, and ETBF or NTBF for 6 h, then changed to serum-free medium for an additional 5 days. Representative tumorsphere images were acquired and the number of tumorspheres (diameter  $\geq$  100  $\mu$ m) was quantified. Scale bar, 100  $\mu$ m. **D**, The expression of stemness markers or maintainers were detected by real-time PCR in cancer cells co-cultured with ETBF. **E**, Western blotting results for NANOG and SOX2 was performed. **F**, The expression of *Nanog* was detected using real-time PCR in organoids obtained from tumors of NTBF/ETBF-gavaged mice in the AOM model. **G**, Representative immunohistochemistry of NANOG protein in xenograft tumor tissues. 400  $\times$  magnifications. Data are expressed as the mean  $\pm$  SEM from three independent experiments. Statistical significance was determined by ANOVA. \*,  $P < .05$ ; \*\*,  $P < .01$ ; \*\*\*,  $P < .001$ .

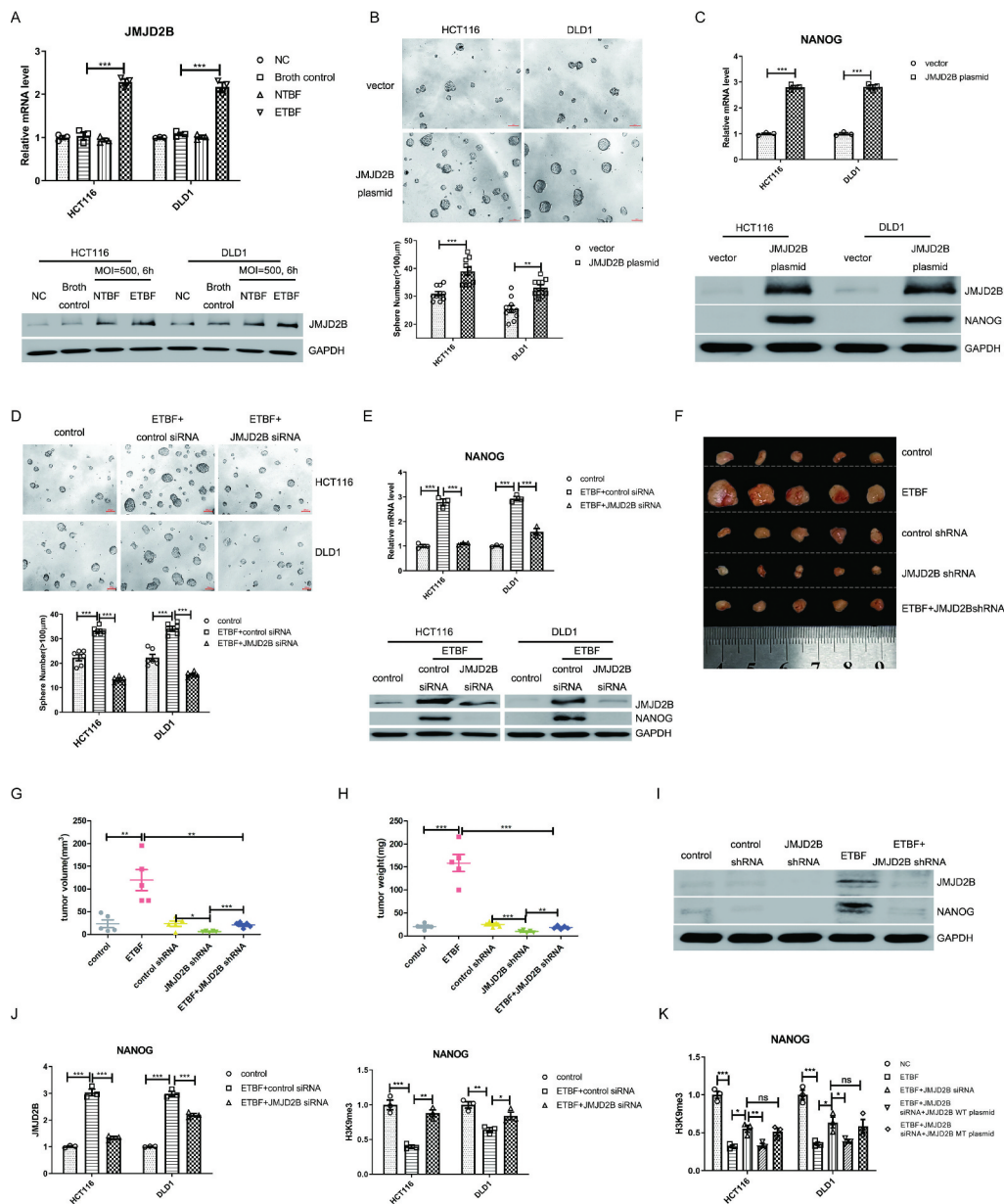


**Figure 2.** JMJD2B epigenetically upregulates NANOG expression to mediate ETBF-induced stemness of CRC cells. **A**, The expression of JMJD2B was measured using real-time PCR and western blotting in CRC cells co-cultured with ETBF. **B**, Representative tumorsphere images were acquired and the number of tumorspheres (diameter  $\geq 100 \mu\text{m}$ ) was quantified in CRC cells (1000 cells/200  $\mu\text{L}$  per well) transfected with the JMJD2B overexpression plasmid. Scale bar, 100  $\mu\text{m}$ . **C**, The effect of JMJD2B plasmid transfection on Nanog expression in HCT116 and DLD1 cells. **D**, ETBF-co-cultured HCT116 and DLD1 cells (1000 cells/200  $\mu\text{L}$  per well) with either scrambled control or JMJD2B siRNA were subjected to tumorsphere formation assay, and the average number of tumorspheres ( $\geq 100 \mu\text{m}$  in diameter) was analyzed. **E**, Knockdown of JMJD2B could abolish the effect of ETBF on the upregulation of NANOG in HCT116 and DLD1 cells. **F**, Representative data of tumors in nude mice bearing HCT116 cells ( $1 \times 10^6$  cells) in different groups.  $N = 5/\text{group}$ . **G** and **H**, Statistical analysis of tumor volume (**G**) and tumor weight (**H**) in different groups,  $n = 5/\text{group}$ . **I**, Western blotting of JMJD2B and NANOG from the representative xenograft tumor tissues in different groups. **J**, Effect of JMJD2B on the occupancies of H3K9me3 in the promoters of NANOG in HCT116 and DLD-1 cells by a ChIP assays (real-time PCR). **K**, Analysis of H3K9 tri-methylation binding to the NANOG promoter in HCT116 and DLD-1 cells to test whether the decrease in H3K9me3 intensity was depended on the lysine de-methylation activity of JMJD2B directly (real-time PCR). Data are expressed as the mean  $\pm$  SEM from three independent experiments. Statistical significance was determined by ANOVA (**A**, **D**, **E**, **G**, **H**, **J** and **K**) and unpaired Student's t test (**B** and **C**). \*,  $P < .05$ ; \*\*,  $P < .01$ ; \*\*\*,  $P < .001$ .

JMJD2B modulated CRC stemness. Tumorsphere cells possess the characteristics of CSCs when compared with the adherent cells; therefore, HCT116 and DLD1 cells were plated in a serum-free suspension culture system to allow tumorsphere formation. As expected, the levels of JMJD2B transcripts and proteins (Supplementary Figure S2 C) were enhanced in the tumorsphere cells compared with those in the adherent cells. Ectopic expression of JMJD2B (Supplementary Fig. S2D) significantly promoted sphere formation (Figure 2B) and increased the expression of NANOG (Figure 2C) in HCT116 and DLD1 cells.

To address whether JMJD2B participates in ETBF-induced stemness, we analyzed the stemness properties in JMJD2B siRNA-transfected CRC cells co-cultured with ETBF. Silencing JMJD2B in the ETBF-infected cells inhibited sphere formation and NANOG expression (Figure 2D,E). The data indicated that ETBF might induce CRC stemness by increasing JMJD2B expression. In addition, the ETBF-induced pro-tumorigenicity effect was reversed by JMJD2B shRNA treatment in tumor-bearing mouse models, as shown by the reduced tumor weight and volume (Figure 2f-H). Moreover, knockdown of JMJD2B blocked ETBF-induced NANOG upregulation in the xenograft tumor tissues (Figure 2I). Thus, these data support the view that ETBF-induced colorectal cancer stemness is dependent on JMJD2B.

As shown in Figure 2E, a higher level of NANOG mRNA was detected in the ETBF-cocultured cells; while downregulation of JMJD2B suppressed the increase in NANOG transcription induced by ETBF. Furthermore, a decrease in the NANOG protein level was detected in JMJD2B-depleted HCT116 and DLD-1 cells co-cultured with ETBF (Figure 2E). In line with this, knockdown of JMJD2B led to a decrease in NANOG expression in the xenograft tumor tissues (Figure 2I). These data indicated that JMJD2B is involved in NANOG regulation in response to ETBF intervention. JMJD2B is a specific demethylase for histone H3K9me3/me2; therefore, we further analyzed the mechanism by which JMJD2B regulates NANOG. ChIP assays (Figure 2J, Supplementary Figure S2E) revealed a significant increase in JMJD2B binding to the NANOG promoter during ETBF infection, while this binding was significantly impaired after

JMJD2B knockdown. Meanwhile, the H3K9me3 levels on the NANOG promoter significantly decreased under ETBF infection conditions and were restored after JMJD2B knockdown. To test whether the decrease in H3K9me3 intensity was catalyzed by JMJD2B directly, the siRNA-resistant JMJD2B wild-type plasmid (JMJD2B-WT) and the H189A/E191Q mutant plasmid (JMJD2B-MT), a catalytically inactive mutant without lysine demethylation activity,<sup>34,35</sup> were transfected into JMJD2B-knockdown cells under ETBF stimulation. In contrast to JMJD2B WT, a nonsignificant change in recruitment was detected in the JMJD2B MT group in JMJD2B-knockdown cells under ETBF stimulation (Figure 2K, Supplementary Figure S2F). These data indicated that JMJD2B-mediated regulation of Nanog is dependent on its demethylase activity.

These results indicated that JMJD2B transactivated NANOG by binding to its promoter and removing the transcriptionally repressive H3K9me3, thus mediated ETBF-induced stemness of CRC cells.

### ***NFAT5 is involved in ETBF-mediated stemness through upregulation of JMJD2B***

To explore the mechanism by which ETBF induces upregulation of JMJD2B at both the mRNA and protein levels, bioinformatic software was used to predict transcription factor binding sites at promoter regions of JMJD2B. We found that the JMJD2B promoter region contained multiple binding sites for NFAT5 (Supplementary Fig. S3A). NFAT5 is a transcription factor that functions as a cell signaling molecule involved in complex adaptive systems. Interaction of lipopolysaccharide (LPS) with host cells through TLRs upregulates the expression of NFAT5.<sup>36</sup> Therefore, we hypothesized that dysregulated NFAT5 expression might contribute to ETBF-increased JMJD2B expression. Real-time PCR and western blotting revealed that exposure of HCT116 and DLD1 cells to ETBF, but not to NTBF, could dramatically increase the expression of NFAT5 (Figure 3A), whereas the mRNA levels of its isoforms, *NFAT c1-c4*, were not significantly affected in both HCT116 and DLD1 cells (Supplementary Fig. S3B). Further, we conducted luciferase reporter assays and

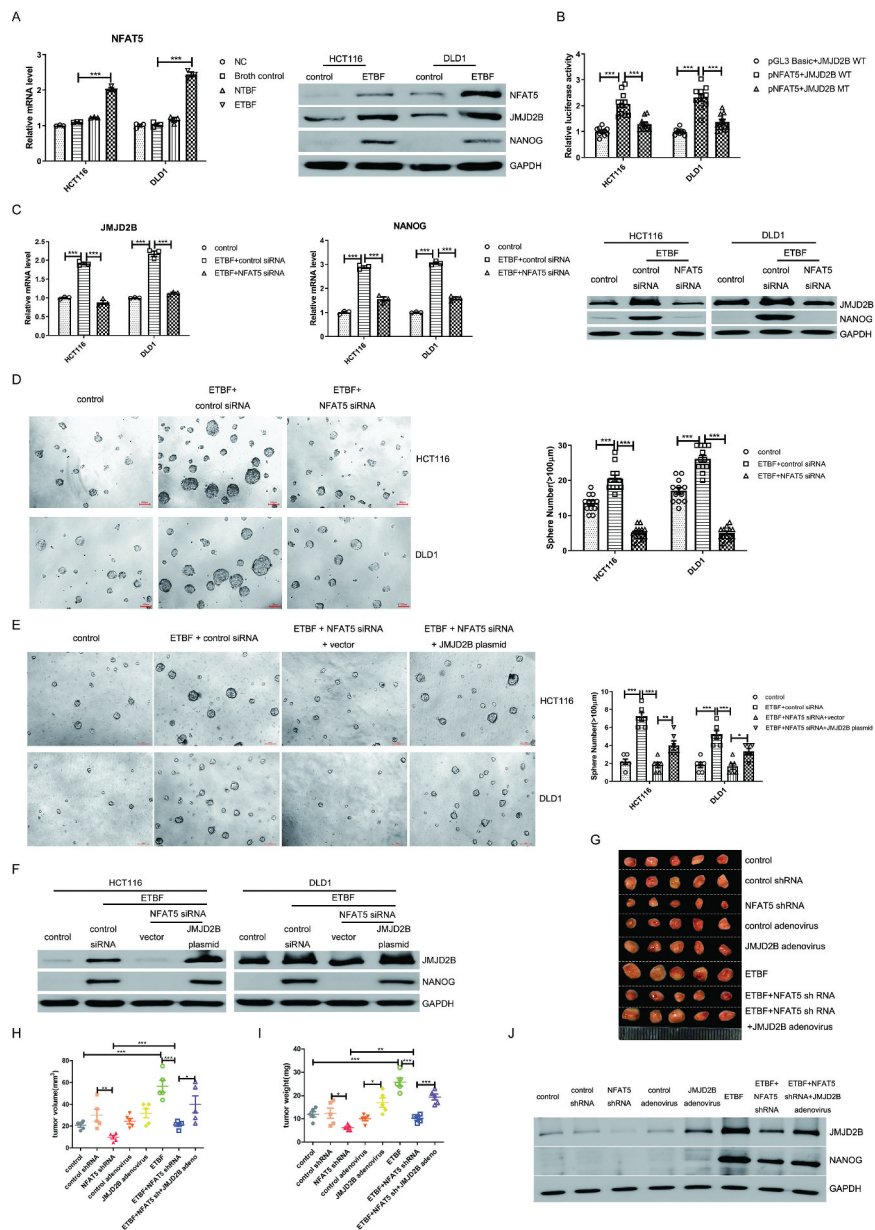


**Figure 3.** ETBF promotes the expression of JMJD2B through NFAT5. **A**, The expression of NFAT5 was measured by real-time PCR and western blotting in CRC cells co-cultured with ETBF (control: Broth control). **B**, Luciferase activity was measured in CRC cells transfected with the *NFAT5* overexpression plasmid or control plasmid. The luciferase JMJD2B recombinant plasmid containing wild-type or mutant binding sites for human *NFAT5* were used. The luciferase activity was normalized based on the control vector transfection. **C**, Real-time PCR and western blotting were performed to detect JMJD2B expression in HCT116 and DLD1 cells. The CRC cells were co-cultured with ETBF and transfected with *NFAT5* siRNA. **D**, ETBF co-cultured HCT116 and DLD1 cells (1000 cells/200  $\mu$ L per well) with either scrambled control or *NFAT5* siRNA were subjected to tumorsphere formation assay, and the average number of tumorspheres ( $\geq 100 \mu$ m in diameter) were analyzed. **E**, The JMJD2B overexpression plasmid transfection could abolish the effect of *NFAT5* siRNA on the reduction of tumorsphere formation in HCT116 and DLD1 cells (500 cells/200  $\mu$ L per well). **F**, Western blotting was performed to detect the expression of NANOG in CRC cells. HCT116 and DLD1 cells were treated with *NFAT5* siRNA, co-cultured with ETBF, and transfected with JMJD2B overexpression plasmid. **G – I**, Representative data of tumors (**G**) in nude mice bearing HCT116 cells ( $1 \times 10^6$  cells) in the different indicated groups. Statistical analysis of tumor volume (**H**) and tumor weight (**I**) in different groups was performed,  $n = 5$ /group. **J**, Western blotting show the level of *NFAT5*, JMJD2B, and NANOG from the representative xenograft tumor tissues in the different indicated groups. Data are expressed as the mean  $\pm$  SEM from three independent experiments. Statistical significance was determined by ANOVA. \*,  $P < .05$ ; \*\*,  $P < .01$ ; \*\*\*,  $P < .001$ .

found that forced overexpression of *NFAT5* notably increased the luciferase activity of HCT116 and DLD1 cells transfected with a wild-type *JMJD2B* recombinant plasmid (*JMJD2B*-WT), but not with the mutant plasmid (*JMJD2B*-MT), which contains no binding sites for *NFAT5* predicted by bioinformatic software (Figure 3B). These data indicated that *NFAT5* could transcriptionally upregulate the expression of *JMJD2B*. Moreover, real-time PCR and western blotting revealed *NFAT5* siRNA dramatically abrogated ETBF-induced upregulation of *JMJD2B* and *NANOG* (Figure 3C and Supplementary Fig. S3 C). In addition, sphere formation was reduced after knocking down *NFAT5* in HCT116 and DLD1 cells co-cultured with ETBF, compared with that in the controls (Figure 3D). This effect was abolished in *JMJD2B* overexpression plasmid-transfected cells (Figure 3E, F).

In the CRC xenograft mouse models, HCT116 cells were inoculated into nude mice, followed by treatment with *NFAT5* shRNA, ETBF co-culture, *JMJD2B* adenovirus, and other treatments. Tumor growth *in vivo* was determined by measuring the tumor volume and weight. As shown in Figure 3G-I, ETBF-induced tumor growth was significantly decreased by knocking down *NFAT5*, and these effects were reversed by *JMJD2B* adenovirus transduction in CRC-bearing nude mice. Furthermore, western blotting confirmed that knockdown of *NFAT5* suppressed ETBF stimulated-*JMJD2B* and *NANOG* expression in the xenograft tumor tissues, and the *NANOG* decrease was efficiently rescued by *JMJD2B* overexpression (Figure 3J). Taken together, these results indicated that *NFAT5* is involved in ETBF-mediated stemness via upregulation of *JMJD2B*, which participates in ETBF-mediated CRC tumorigenesis.

### **ETBF induces CRC stemness through selectively activating the Toll-Like 4 pathway**

The TLR signaling pathway is activated in response to *Bacteroides fragilis* (*B. fragilis*) intervention.<sup>37,38</sup> Consistent with these findings, we found that TLR4 was highly expressed after ETBF infection (Figure 4A), whereas the mRNA levels of other *TLRs* that are located on the cell membrane were not notably affected (data not shown). To examine whether

TLR4 participates in ETBF-induced stemness, we transfected CRC cells with TLR4 siRNA and co-cultured the cells with ETBF. We found that knockdown of TLR4 significantly reduced the formation of ETBF-induced tumorspheres and abolished the effect of ETBF on *NFAT5*, *JMJD2B*, and *NANOG* expression (Figure 4B, C). Moreover, ectopic expression of *NFAT5* or *JMJD2B* in HCT116 and DLD1 cells significantly reversed the TLR4 siRNA-impaired stemness and dramatically attenuated the reduction of *JMJD2B* and *NANOG* expression caused by the TLR4 siRNA (Figure 4D-G). Furthermore, ETBF-induced tumorigenesis was suppressed by knocking down TLR4 in the CRC xenograft mouse model, as shown by reduced tumor weight and tumor volume (Figure 4H-J). In addition, knockdown of TLR4 downregulated *NFAT5*, *JMJD2B*, and *NANOG* expression in the xenograft tumor tissues (Figure 4K).

Taken together, these data suggested that the stemness-promoting effect of ETBF depends, at least in part, on TLR4 activation.

### **The levels of ETBF, NFAT5, JMJD2B, and NANOG correlate with in patients with CRC**

Given the interplay among ETBF, *NFAT5*, and *JMJD2B*, and their potential causal link to colorectal tumorigenesis in mouse models, we further tested these results in tissues from 56 CRC patients we studied above. The mRNA expression of *NFAT5*, *JMJD2B*, and *NANOG* significantly increased in the ETBF-high group (Figure 5A). Pearson rank sum test further showed that ETBF in CRC tissues correlated positively with *NFAT5*, *JMJD2B*, and *NANOG* (Figure 5B); *NFAT5* moderately correlated with *JMJD2B* and *NANOG* (Figure 5C). Thus, we demonstrated a link among ETBF, *NFAT5*, and *JMJD2B* and stemness in colorectal tumorigenesis.

### **Discussion**

In the current study, we provided evidence that ETBF upregulates histone demethylase *JMJD2B* via a TLR4-*NFAT5*-dependent pathway, playing an important role in the stemness, which promotes colorectal carcinogenesis. Inhibition of *JMJD2B* expression *in vitro* and *in vivo* impairs ETBF-induced CSCs properties, through directly binding to and removing transcriptional repressive H3K9me3 marks on the *NANOG*



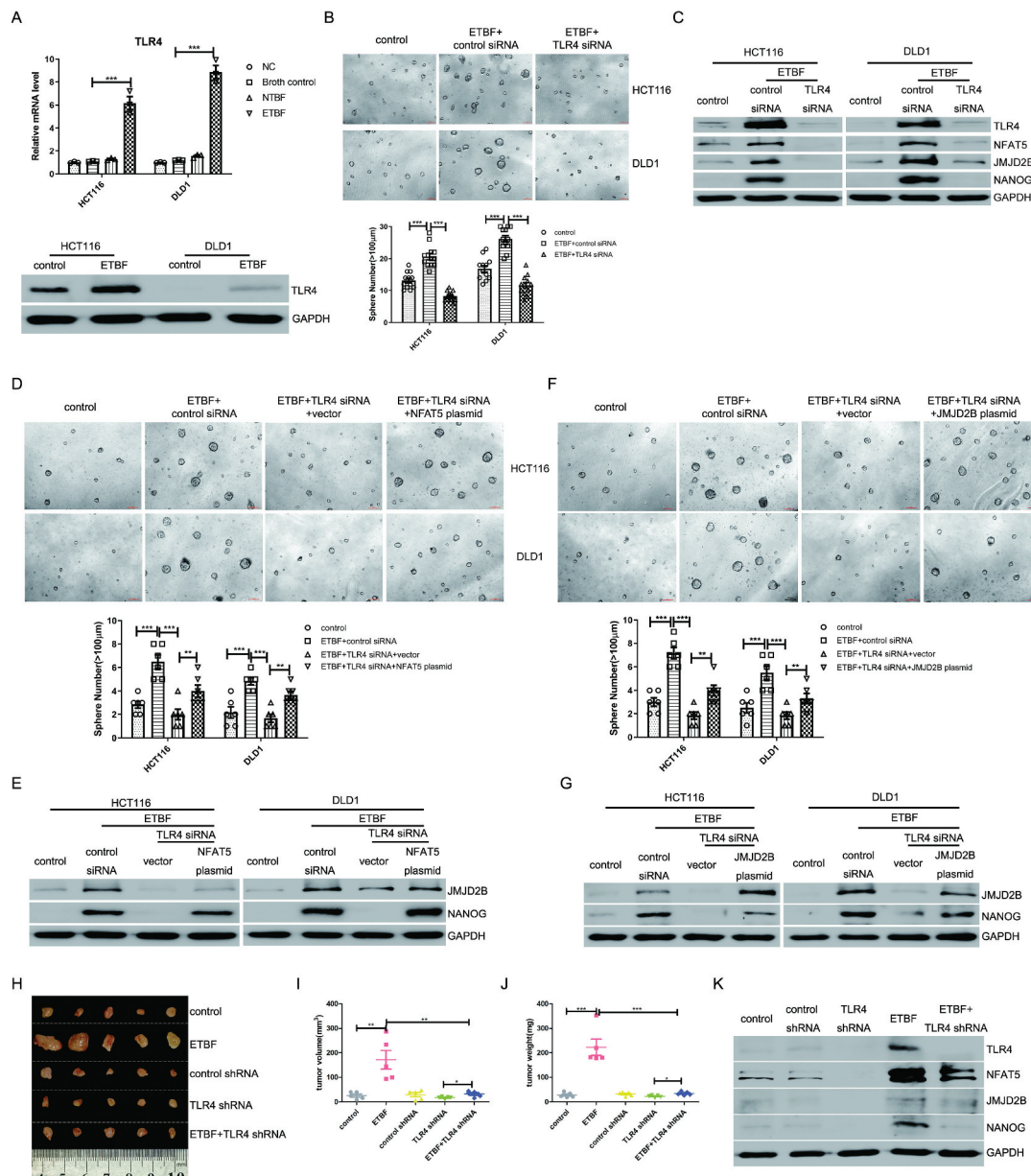


**Figure 4.** ETBF induces CRC cells stemness through Toll-like receptor 4 (TLR4). **A**, Real-time PCR and western blotting of TLR4 in HCT 116 and DLD1 cells co-cultured with ETBF (control: Broth control). **B**, ETBF-co-cultured HCT116 and DLD1 cells (500 cells/200  $\mu$ L per well) with either scrambled control or TLR4 siRNA were subjected to tumorsphere formation assay, and the average number of tumorspheres ( $\geq 100 \mu$ m in diameter) was analyzed. **C**, Western blotting showing the levels of NFAT5, JMJD2B, and NANOG in HCT 116 and DLD1 cells co-cultured with ETBF and transfected with TLR4 siRNA. **D**, NFAT5 overexpression plasmid transfection could abolish the effect of TLR4 siRNA on the reduction of tumorsphere formation in HCT116 and DLD1 cells (500 cells/200  $\mu$ L per well). **E**, Western blotting was performed to detect the levels of JMJD2B and NANOG in CRC cells. HCT116 and DLD1 cells were treated with TLR4 siRNA, co-cultured with ETBF, and transfected with the NFAT5 overexpression plasmid. **F**, Tumorsphere formation assays were performed. HCT116 and DLD1 cells (500 cells/200  $\mu$ L per well) were treated with TLR4 siRNA, co-cultured with ETBF, and transfected with JMJD2B overexpression plasmid. **G**, Western blotting was performed to detect the expression of NANOG. HCT116 and DLD1 cells were treated with TLR4 siRNA, co-cultured with ETBF, and transfected with JMJD2B overexpression plasmid. **H – J**, Representative data of tumors (**H**) in nude mice bearing HCT116 cells ( $1 \times 10^6$  cells) in different indicated groups. Statistical analysis of tumor volume (**I**) and tumor weight (**J**) in different groups was performed,  $n = 5/\text{group}$ . **K**, Western blotting showed the levels of TLR4, NFAT5, JMJD2B, and NANOG from the representative xenograft tumor tissues in different indicated groups. Data are expressed as the mean  $\pm$  SEM from three independent experiments. Statistical significance was determined by ANOVA. \*\*,  $P < .01$ ; \*\*\*,  $P < .001$ .



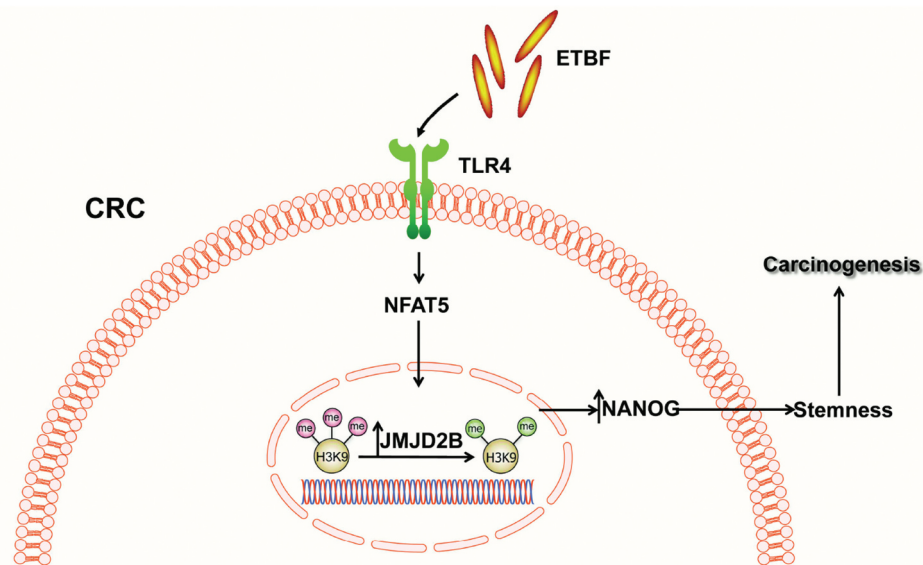


**Figure 6.** Schematic representation of ETBF-induced stemness in colorectal cancer via upregulating JMJD2B.

the stemness of CRC cells using a sphere-forming assay. Stemness maintainers NANOG and SOX2 were greatly induced in ETBF-infected cells. Accordingly, treatment with ETBF increased the growth and the size of tumor organoids compared with those of the controls. Although several studies have demonstrated that the microbiota within the tumor microenvironment, such as acidophilic bacteria, *E. faecalis*, or nonpathogenic *E. coli*, could increase the stem cell activity of CRC, our data shows, for the first time, a potential causal link between ETBF and CRC development.

We subsequently explored the molecular mechanism by which ETBF induces CRC cells stemness. Changes in the intestinal microenvironment, such as dysbacteriosis, can cause histone modifications and chromatin structure alterations by recruiting or retrieving chromatin-modifying enzymes.<sup>40,41</sup> H3K9me3 is a hallmark of gene transcriptional repression regions. Expression activation of the stemness maintainers NANOG and SOX2 are regulated by H3K9me3 demethylation.<sup>42,43</sup> The histone demethylase JMJD2 is the only member of gene family that can remove H3K9me3, and its members include JMJD2A, JMJD2B, JMJD2C, and JMJD2D. Compelling evidence indicates that JMJD2B is overexpressed in human CRC tissue, and that it is implicated in various cellular processes, including apoptosis, cell cycle,

invasion, DNA damage response, and metabolism to promote CRC progression.<sup>44–47</sup> Furthermore, JMJD2B plays a critical role in self-renewal of ESCs and iPSC generation.<sup>48,49</sup> Consequently, we hypothesized that ETBF promotes CRC stemness via JMJD2B. In support of this, we found that genetic inhibition of JMJD2B in ETBF-co-cultured cells inhibited sphere formation and NANOG expression. Furthermore, ETBF-induced pro-tumorigenicity effect was reversed using JMJD2B shRNA in the tumor bearing mouse models. ChIP data revealed high occupancies of H3K9me3 in the promoters of NANOG, and JMJD2B could transcriptionally upregulate the expression of NANOG by binding and removing the inhibitory H3K9me3 in the NANOG promoter region.

We also uncovered the mechanisms by which ETBF mediates JMJD2B upregulation. We used bioinformatics software to analyze the *JMJD2B* promoter sequence in detail and found that it contained multiple NFAT5 transcription factor binding sites, suggesting that NFAT5 is involved in the transcriptional regulation of *JMJD2B*. NFAT5 and NF- $\kappa$ B belong to the Rel family of proteins, which were first discovered in T cells. Subsequent studies have found that many tissues express NFAT5, such as the brain, kidney, and lung.<sup>50</sup> In recent years, researchers have found that the function of NFAT5 is not limited to the renal medulla. This suggests that

NFAT5 might also be involved in embryonic formation and development, liver detoxification, and tumor metastasis.<sup>51–54</sup> Our functional studies revealed that NFAT5 targets JMJD2B, is selectively activated because of ETBF co-culture, and can biologically modulate CRC stemness *in vitro* and *in vivo*. Considering that the TLR signaling pathway is essential for *B. fragilis* infection,<sup>55–57</sup> we demonstrated that the ETBF-induced genomic activation of NFAT5, JMJD2B, and NANOG depends on TLR4. Therefore, ETBF orchestrates TLR4, NFAT5, JMJD2B, and NANOG networks to exert biological control of CRC stemness. The potential virulence factors of *B. fragilis* which have been identified contain capsular polysaccharides (A–H),<sup>58,59</sup> Lipopolysaccharide (LPS)<sup>60,61</sup> and BFT.<sup>5</sup> Recent studies have shown that the biological activities of *B. fragilis*-derived Polysaccharide A (PSA) and LPS are mediated by TLR4 activation.<sup>60,62</sup> Similarly, Ahmadi et al. reported that *B. fragilis* and *B. fragilis*-derived outer membrane vesicles (OMVs, which contain bacterial components including LPS, outer membrane proteins, phospholipids, periplasmic components, DNA, RNA, hydrolytic enzymes and signaling molecules) both increase the mRNA levels of TLR4.<sup>57</sup> BFT, key virulence factor of ETBF, binds to an uncharacterized cell surface receptor,<sup>63,64</sup> triggering an array of signal transduction and contributing to key aspects of ETBF carcinogenic potential. However, until now, researchers have found that BFT may not directly induce Toll-like receptor activation.<sup>65</sup> In our study, we stimulated HCT116 and DLD1 cells with ETBF and their mixed culture medium, which contain all potential virulence factors. Whether the ETBF-induced TLR4 activation is dependent on LPS, PSA, BFT or other identified/unidentified factors, awaits future studies.

In summary, our findings revealed that ETBF might act on CRC tumorigenesis via upregulating TLR4 and NFAT5, which subsequently transcriptionally upregulate JMJD2B, which increases NANOG expression by specifically demethylating promoter repressive H3K9me3, consequently promoting the CRC cells stemness. The current study provides a rationale for detecting and treating ETBF and identified JMJD2B as a promising anti-CRC target.

## Materials and methods

### Patient specimens

Patients were diagnosed pathologically with CRC. The collection of CRC tissues was approved by the ethics committee of Renji Hospital, Shanghai Jiao Tong University School of Medicine (Shanghai, China). Informed consent was obtained from patients with CRC before sample collection in accordance with institutional guidelines. The relevant clinical and histopathological characteristics provided to the researchers were anonymized. All experiments were carried out in accordance with the provisions of the Helsinki Declaration of 1975.

### Cell lines, bacterial strains, plasmids, and adenovirus

Human CRC cell lines HCT116 and DLD1 (ATCC, Manassas, VA, USA) were cultured in RPMI-1640 medium (Gibco, Grand Island, NY, USA) supplemented with 10% fetal bovine serum (FBS, Gibco). All cell lines were genotyped for identity by Beijing Microread Genetics Co., Ltd. Routine Mycoplasma testing was performed by MycoAlert Mycoplasma Detection Kit (Lonza, Basel, Switzerland, LT07-118) every 3 to 6 months. Cell lines were grown for no more than 10 passages in all experiments. Bacterial strains, nontoxigenic *Bacteroides fragilis* (NTBF, ATCC 25285), ETBF (ATCC 43860), *Fusobacterium nucleatum* (ATCC 25586), and *Clostridium symbiosum* (ATCC 14940) were cultured at 37 °C under anaerobic conditions (DG250, Don Whitley Scientific, West Yorkshire, UK) in brain heart infusion (BHI) broth supplemented with Yeast Extract, K<sub>2</sub>HPO<sub>4</sub>, Resazurin, L-cysteine, hemin, and Vitamin K1.<sup>65</sup> Commensal *E. coli* strain DH5α (CB101, Tiangen, Beijing, China) was cultured in Luria-Bertani medium for 12–16 h at 37 °C in shake cultivation at 220 rpm/min. For a single treatment, HCT116 and DLD1 cells were exposed to NTBF, ETBF, *F. nucleatum*, *C. symbiosum*, and *E. coli*, respectively, in penicillin/streptomycin-free RPMI-1640 (multiplicity of infection = 500) for 6 h. After 6 h, the medium containing bacterial strains was replaced with conventional cell culture medium. Plasmids pCMV-HA-NFAT5 and pCMV-HA-JMJD2B (wide-type and mutant) were purchased from Genechem (Shanghai, China). Short hairpin RNA (shRNA)

adenovirus constructs targeting TLR4, NFAT5, and JMJD2B, and overexpression adenovirus constructs for JMJD2B were purchased from OBiO Technology (Shanghai, China).

### Antibodies

Primary antibodies used were anti-TLR4 (Abcam, Cambridge, MA, USA, ab13556), anti-NFAT5 (Abcam, ab3446), anti-JMJD2B (Bethyl Laboratories, Montgomery, TX, USA, A301-478), anti-NANOG (Cell Signaling Technology, Danvers, MA, USA, 3580 S; Abcam, ab80892), anti-GAPDH (Kangcheng, Shanghai, China, 5G5), and anti-histone H3 (trimethyl K9) (Abcam, ab8898). Horseradish peroxidase (HRP)-conjugated goat anti-rabbit IgG (H + L) (Kangcheng; RB-035) was used as the secondary antibody.

### Sphere forming assay<sup>66</sup>

Cells were trypsinized and plated onto Costar® 96-well Ultra-low attachment plates in serum-free medium consisting of serum-free Dulbecco's modified Eagle's medium (DMEM)/F12 (Gibco) with 1% B27 nutrient mixture (Thermo Fisher Scientific, Waltham, MA, USA) plus 20 ng/mL epidermal growth factor, 10 ng/mL fibroblast growth factor, 5 µg/mL insulin, and 0.4% bovine serum albumin. Formation of sphere-like structures was visible after 2 days, and images of each group were captured after 5 days. The number of spheres (diameter ≥ 100 µm) was calculated using Image J software (NIH, Bethesda, MD, USA).

### RNA isolation, cDNA synthesis, and real-time PCR analysis

Total RNA was isolated using the TriZol Reagent (Life Technologies, Carlsbad, CA, USA) in accordance with the manufacturer's instructions. For cDNA synthesis, 2 µg of quantified RNA was reverse transcribed using an SuperScript RT Reagent II Kit (Takara, Kusatsu, Shiga, Japan). Primers for qPCR were designed using PrimerBank or referred from the literature (Table 2). Real-time PCR was performed using a TB Green™ Premix Ex Taq™ II kit (Takara) on a StepOnePlus Real-Time PCR System (Applied Biosystems, Carlsbad, CA, USA). Gene expression was quantified by real-time PCR using *GAPDH* and 16 s RNA as housekeeping controls. The differential fold change in gene expression was calculated using the  $2^{(-\Delta\Delta Ct)}$  method.<sup>67</sup>

### Protein isolation and western blotting

Whole cell lysates were prepared by adding Radioimmunoprecipitation assay (RIPA) lysis buffer (Beyotime, Shanghai, China) with a protease inhibitor cocktail (Kangcheng). For xenograft tumor lysate preparation, snap frozen tumors were homogenized using a high-throughput tissue grinder (WonBio, Shanghai, China) before adding lysis buffer. Isolated total proteins were quantified using a bicinchoninic acid (BCA) Protein Assay Kit (Thermo Fisher Scientific), and equal amounts of lysates were resolved in appropriate SDS-PAGE gels, transferred onto 0.45-µm polyvinylidene fluoride (PVDF) membranes (Millipore, Bangalore, India), and then probed with primary antibodies. HRP-conjugated secondary antibodies and Supersignal West Pico chemiluminescent substrate (Thermo Fisher Scientific) were used for immunoreactive protein band detection using the ChemiDoc™ Imaging System (BIO-RAD, Hercules, CA, USA). GAPDH was used as the protein loading and transfer control.

### RNA interference

Small interfering RNAs (siRNAs) specifically targeting TLR4, NFAT5, and JMJD2B were purchased from GenePharma (Shanghai, China) using the following sequences: JMJD2B: siRNA-1, 5'-GCGCAGAAUCUACCAACUU-3' and siRNA-2, 5'-CAAAUACGUGGCCUACAUA-3'. These siRNAs were used as a pool for siRNA transfection. The other siRNAs were TLR4 siRNA: 5'-GCCGAAAGGUG

AUUGUUGUTT-3'; and NFAT5 siRNA: 5'-GCAACACAGTTTCAGACAA-3'. HCT116 and DLD1 cells were seeded at 30% confluence in six-well plates overnight before transfection and then transfected with 100 nM siRNA using the Lipofectamine™ 2000 Transfection Reagent (Thermo Fisher Scientific) in accordance with the manufacturer's instructions. A nonspecific siRNA was used as a negative control.

### Chromatin immunoprecipitation (ChIP) assays

ChIP assays were conducted in accordance with the manufacturer's protocol (Millipore). Briefly, cells were incubated with 1% formaldehyde for 10–15 min at 37°C. The cells were then lysed and sonicated. The samples were centrifuged at 13,000 rpm. The diluted supernatant was pre-cleared using 75 µL of protein A agarose beads.

**Table 2.** Primers used for PCR and real-time PCR.

Gene		Sequence	Product length (bp)
h <i>GAPDH</i>	Forward	GCATTGCCCTCAACGACCAC	78
	Reverse	CCACCACCCTGTTGCTGTAG	
h <i>CD133</i>	Forward	GGTCTGGCGAGCTAAGGGAA	217
	Reverse	GGGGAAGGCAAGCGTGTT	
h <i>CD44</i>	Forward	TTTGCAATTGCAGTCAACAGTC	234
	Reverse	GTTACACCCCAATCTTCATGTCCAC	
h <i>LGR5</i>	Forward	TATGCCTTTGAAAACCTCTC	262
	Reverse	CACCATTGAGAGTCAGTGTT	
h <i>NANOG</i>	Forward	TCCAGCAGATGCAAGAAGCTCTCCA	131
	Reverse	CACACCATTGCTATTCTTCGGCCA	
h <i>OCT4</i>	Forward	TCAGCTTCTCCACCACCT	103
	Reverse	TATTCAGCCAAAACGACCATCT	
h <i>SOX2</i>	Forward	ATGACCAGCTCGCAGACCTAC	107
	Reverse	TTGACCACCGAACCATGGAG	
h <i>JMJD2B</i>	Forward	TCACCAGCCACATCTACCAG	68
	Reverse	GATGTCCCCACGCTTAC	
h <i>NANOG</i> (for ChIP)	Forward	AGAAGTATTTGTTGCTGGGTTGTCTTCAGG	199
	Reverse	GGCTCTATCACCTTAGACCCACC	
h <i>NFAT c1</i>	Forward	CTGCAGGACTCCAAGGTCAT	119
	Reverse	GGGATCTCAACCACAGAGA	
h <i>NFAT c2</i>	Forward	ACCAGGAGTCCAGCACATC	124
	Reverse	TGCTGAATGACTGTGGGGTA	
h <i>NFAT c3</i>	Forward	AGTCCATCTTTGCCTGTGC	123
	Reverse	TATGTTTGTGGGATGGAGCA	
h <i>NFAT c4</i>	Forward	GGGCCACTATGAGACAGAA	120
	Reverse	TGCCGATGAACATCTGTAGG	
h <i>NFAT 5</i>	Forward	CAAAGCCAACAAGGAACCAT	124
	Reverse	GTTGTTGTTGCTGCTGTGT	
h <i>TLR4</i>	Forward	AGACCTGCCCTGAACCCAT	147
	Reverse	CGATGGACTTCTAAACCAGCCA	
m <i>Gapdh</i>	Forward	TGACCTCAACTACATGGTCTACA	85
	Reverse	CTTCCATTCTCGGCCTTG	
m <i>Nanog</i>	Forward	CACAGTTTGCCTAGTTCTGAGG	86
	Reverse	GCAAGAATAGTTCTCGGGATGAA	
16 s	Forward	GGTGAATACGTTCCCGG	145
	Reverse	TACGGCTACCTGTTACGACTT	
<i>bft</i>	Forward	GACGGTGTATGTGATTTGCTGAGAGA	294
	Reverse	ATCCCTAAGATTTTATTATCCCAAGTA	
NTBF	Forward	TTCAACCTGATCGATCCGGGAAGATCCG	1600
	Reverse	GCTGGTAGACTACTCTGAGTAAGGAGTC	

Then, the anti-JMJD2B and anti-H3K9me3 antibodies were immunoprecipitated with the cross-linked mixture overnight at 4°C. After a series of washes, the crosslinking was reversed and purified for PCR and real-time PCR analysis. The primer sequences for the human *NANOG* promoter for ChIP are shown in Table 2.

#### Dual-luciferase reporter assay

Sub-confluent HCT116 and DLD1 cells were seeded in 96-well plates and co-transfected with luciferase reporter plasmids expressing *NFAT5*, *JMJD2B* (wild-type and mutant), and Renilla luciferase (Generay, Shanghai, China). After incubation for 24 h, the cells were lysed and subjected to luciferase assays using the Dual-Luciferase Reporter Assay System (Promega, Madison, WI, USA) and FLUOstar® Omega multi-mode microplate reader (BMG Labtech, Offenburg, Germany).

#### AOM murine model

Conventional male C57BL/6 mice were bred in the Animal Laboratory at the Renji Hospital, Shanghai Jiao Tong University School of Medicine. In the mouse model of azoxymethane (AOM, Sigma-Aldrich, St Louis, MO, USA)-induced colorectal tumorigenicity, we gave antibiotics to the mice through drinking water, comprising 0.2 g/L ampicillin, neomycin, and metronidazole, and 0.1 g/L vancomycin (Sigma-Aldrich) daily for 2 weeks. After the last dose of antibiotics, the mice were injected with AOM intraperitoneally (10 mg/kg, once a week for 10 weeks) and gavaged with  $1 \times 10^9$  colony forming units (CFU) of NTBF or ETBF twice weekly for 20 weeks. The mice were killed 3 days after the last gavage.

#### Xenografts in nude mice

Five-week-old male BALB/c nude mice were housed under specific pathogen-free (SPF) conditions. To

evaluate the role of ETBF in regulating stemness *in vivo*,  $1 \times 10^5$ ,  $5 \times 10^5$ , and  $1 \times 10^6$  HCT116 cells were injected subcutaneously to establish separate CRC xenograft models. In the subsequent xenograft experiments,  $1 \times 10^6$  HCT116 cells were injected subcutaneously. One week after subcutaneous inoculation, the mice were randomly divided into different groups for different sets of experiments. The relevant viral vectors and ETBF (multiplicity of infection = 500) were given via multipoint intratumoral injection, twice a week for three weeks.

Tumor volumes were calculated as follows: (longest diameter)  $\times$  (shortest diameter)<sup>2</sup>  $\times$  0.5. At the end point, the tumors were dissected and analyzed. All animal studies were conducted in accordance with the guidelines published in the Animal Ethics Committee.

### Immunohistochemistry

Tumor tissues were fixed in 4% paraformaldehyde at room temperature for 24 h and then embedded in paraffin. Samples were cut into 4- $\mu$ m sections, deparaffined, and then rehydrated. Endogenous peroxidase activity was quenched with 3% H<sub>2</sub>O<sub>2</sub> for 10 min, and the sections were washed and heated by a microwave in citrate buffer (Maxim, Fujian, China) for antigen retrieval. Then, sections were blocked with horse serum (Maxim) for 30 min and incubated with primary antibodies against NANOG at 4°C overnight and HRP-conjugated polyclonal anti-mouse/rabbit antibodies (Maxim) at room temperature for 30 min. Sections were developed with DAB buffer (Maxim) using standard protocols.

### Generation and propagation of organoid cell cultures<sup>68</sup>

Isolated colorectal tumors from C57BL/6 mice were trypsinized for single-cell culture, mixed with Matrigel (Corning, NY, USA), and then placed in 24-well plates at 15000 cells per 50  $\mu$ L of Matrigel per well. The Matrigel was allowed to polymerize at 37°C, and then basal culture medium (advanced DMEM/F12, Gibco) containing 1 U/mL penicillin (Gibco), 1  $\mu$ g/mL streptomycin (Gibco), 10 mmol/L HEPES (Gibco), 2 mM Glutamax (Gibco), 1  $\times$  N2 supplement (Gibco), 1  $\times$  B27 supplement (Gibco), 50 ng/mL of murine EGF (Gibco), and 2.5 ng/mL amphotericin B

(Sigma-Aldrich), 1 mmol/L N-acetylcysteine (Sigma-Aldrich). The culture medium was changed every 2 days, and organoids were passaged at 1:5 once a week.

### Detection of the total bacteria, NTBF, and ETBF in mice stool samples

*Bacteroides fragilis* toxin gene (*bft*) was used to identify oncogenic ETBF. The primer sequences for NTBF, ETBF (*bft*) and 16 s are described in Table 2. Genomic DNA was extracted from mouse stool samples of equal weight using a QIAamp PowerFecal DNA Kit (QIAGEN, Hilden, Germany). DNA from each specimen was subjected to PCR to determine the amounts of total bacteria, NTBF, and ETBF. Each reaction contained 100 ng of DNA and was assayed in triplicate.

### Detection of ETBF in human CRC tissue

Genomic DNA was extracted from human CRC tissue using a QIAamp Fast DNA Tissue Kit (QIAGEN) and subjected to real-time PCR to determine the amounts of ETBF. The primer sequences of ETBF (*bft*) and 16 s are described in Table 2. Each reaction contained 100 ng of DNA and was assayed in triplicate.

### Statistical analysis

All statistical analysis were performed using GraphPad Prism6 software (GraphPad Software, Inc. La Jolla, CA, USA). Independent sample t test (unpaired Student's t test and Mann-Whitney test) was conducted for the comparison of two conditions. Analysis of variance (ANOVA) was used for multiple comparisons. Wilcoxon's rank-sum test was performed to evaluate the correlations of ETBF abundance, and *NFAT5*, *JMJD2B*, and *NANOG* levels. The  $\chi^2$ -test was used to evaluate the correlation between ETBF abundance and the clinicopathological factors of patients with CRCs. Values were considered significantly different at  $P < .05$  and expressed as the mean  $\pm$  SEM from three independent experiments.

### Disclosure of potential conflicts of interest

All authors declare that there are no conflicts of interest.

## Funding

This study was supported by the National Natural Science Foundation of China (No. 81772506, 81530072, 81972203, 81802321), the funds from Shanghai Shenkang Center (SHDC12018121), and Shanghai Municipal Education Commission–Gaofeng Clinical Medicine Grant Support (No. 20152210).

## Author contributions

**Conception and design:** Q.- Q. Liu, Y.- X. Chen.

**Development of methodology:** Q.- Q. Liu, C.- M. Li, L.- N. Fu, Q.-Y. Gao, Y.- X. Chen.

**Acquisition of data (provided animals, acquired and managed patients, provided facilities, etc.):** Q.- Q. Liu, C.- M. Li, L.- N. Fu, H.- L. Wang.

**Analysis and interpretation of data (e.g., statistical analysis, biostatistics, computational analysis):** Q.- Q. Liu, C.- M. Li, L.- N. Fu, H.- L. Wang, J. Tan, Y.- Q. Wang, D.- F. Sun, Q.-Y. Gao.

**Writing, review, and/or revision of the manuscript:** Q.- Q. Liu, Y.-X. Chen, J.-Y. Fang.

**Administrative, technical, or material support (i.e., reporting or organizing data, constructing databases):** L.- N. Fu, D.- F. Sun, Q.-Y. Gao.

**Study supervision:** Y.-X. Chen, J.-Y. Fang.

## References

1. Cartwright TH. Treatment decisions after diagnosis of metastatic colorectal cancer. *Clin. Colorectal Cancer*. 2012;11(3):155–166. doi:10.1016/j.clcc.2011.11.001.
2. Siegel R, Naishadham D, Jemal A. Cancer statistics, 2013. *CA Cancer J. Clin.* 2013;63(1):11–30. doi:10.3322/caac.21166.
3. Boleij A, Hechenbleikner EM, Goodwin AC, Badani R, Stein EM, Lazarev MG, Ellis B, Carroll KC, Albesiano E, Wick EC, et al. The *Bacteroides fragilis* toxin gene is prevalent in the colon mucosa of colorectal cancer patients. *Clin Infect Dis*. 2015;60(2):208–215. doi:10.1093/cid/ciu787.
4. Prindiville TP, Sheikh RA, Cohen SH, Tang YJ, Cantrell MC, Jr SJ. *Bacteroides fragilis* enterotoxin gene sequences in patients with inflammatory bowel disease. *Emerg Infect Dis*. 2000;6(2):171–174. doi:10.3201/eid0602.000210.
5. Toprak NU, Yagci A, Gulluoglu BM, Akin ML, Demirkalem P, Celenk T, Soyletir G. A possible role of *Bacteroides fragilis* enterotoxin in the aetiology of colorectal cancer. *Clin Microbiol Infect*. 2006;12(8):782–786. doi:10.1111/j.1469-0691.2006.01494.x.
6. Legakis NJ, Ioannides H, Tzannetis S, Golematis B, Papavassiliou J. Faecal bacterial flora in patients with colon cancer and control subjects. *Zentralbl Bakteriell Mikrobiol Hyg A*. 1981;251:54–61.
7. Dejea CM, Fathi P, Craig JM, Boleij A, Taddese R, Geis AL, Wu X, DeStefano Shields CE, Hechenbleikner EM, Huso DL. Patients with familial adenomatous polyposis harbor colonic biofilms containing tumorigenic bacteria. *Science*. 2018;359(6375):592–597. doi:10.1126/science.aah3648.
8. Wu S, Powell J, Mathioudakis N, Kane S, Fernandez E, Sears CL. *Bacteroides fragilis* enterotoxin induces intestinal epithelial cell secretion of interleukin-8 through mitogen-activated protein kinases and a tyrosine kinase-regulated nuclear factor-kappaB pathway. *Infect Immun*. 2004;72(10):5832–5839. doi:10.1128/IAI.72.10.5832-5839.2004.
9. Wu S, Morin PJ, Maouyo D, Sears CL. *Bacteroides fragilis* enterotoxin induces c-Myc expression and cellular proliferation. *Gastroenterology*. 2003;124(2):392–400. doi:10.1053/gast.2003.50047.
10. Goodwin AC, Destefano Shields CE, Wu S, Huso DL, Wu X, Murray-Stewart TR, Hacker-Prietz A, Rabizadeh S, Woster PM, Sears CL, et al. Polyamine catabolism contributes to enterotoxigenic *Bacteroides fragilis*-induced colon tumorigenesis. *Proc Natl Acad Sci U S A*. 2011;108(37):15354–15359. doi:10.1073/pnas.1010203108.
11. Kim JM, Lee JY, Kim YJ. Inhibition of apoptosis in *Bacteroides fragilis* enterotoxin-stimulated intestinal epithelial cells through the induction of c-IAP-2. *Eur J Immunol*. 2008;38(8):2190–2199. doi:10.1002/eji.200838191.
12. Wu S, Rhee K-J, Albesiano E, Rabizadeh S, Wu X, Yen H-R, Huso DL, Brancati FL, Wick E, McAllister F, et al. A human colonic commensal promotes colon tumorigenesis via activation of T helper type 17 T cell responses. *Nat Med*. 2009;15(9):1016–1022. doi:10.1038/nm.2015.
13. Chung L, Thiele Orberg E, Geis AL, Chan JL, Fu K, DeStefano Shields CE, Dejea CM, Fathi P, Chen J, Finard BB, et al. *Bacteroides fragilis* toxin coordinates a pro-carcinogenic inflammatory cascade via targeting of colonic epithelial cells. *Cell Host Microbe*. 2018;23(2):203–214. doi:10.1016/j.chom.2018.01.007.
14. Batlle E, Clevers H. Cancer stem cells revisited. *Nat Med*. 2017;23:1124–1134. doi:10.1038/nm.4409.
15. Visvader JE. Cells of origin in cancer. *Nature*. 2011;469:314–322. doi:10.1038/nature09781.
16. Wahab SMR, Islam F, Gopalan V, Lam AK, Identifications T. Clinical implications of cancer stem cells in colorectal cancer. *Clin Colorectal Cancer*. 2017;16(2):93–102. doi:10.1016/j.clcc.2017.01.011.
17. Saigusa S, Tanaka K, Toiyama Y, Yokoe T, Okugawa Y, Ioue Y, Miki C, Kusunoki M. Correlation of CD133, OCT4, and SOX2 in rectal cancer and their association with distant recurrence after chemoradiotherapy. *Ann Surg Oncol*. 2009;16(12):3488–3498. doi:10.1245/s10434-009-0617-z.
18. Elbadawy M, Usui T, Yamawaki H, Sasaki K. Emerging roles of C-Myc in cancer stem cell-related signaling and



- resistance to cancer chemotherapy: a potential therapeutic target against colorectal cancer. *Int J Mol Sci*. 2019;20(9):pii: E2340. doi:10.3390/ijms20092340.
19. Hu Y-B, Yan C, Mu L, Mi Y-, Zhao H, Hu H, Li X-L, Tao -D-D, Wu Y-Q, Gong J-P. Exosomal Wnt-induced dedifferentiation of colorectal cancer cells contributes to chemotherapy resistance. *Oncogene*. 2019;38(11):1951–1965. doi:10.1038/s41388-018-0557-9.
  20. Guo P, Wang J, Gao W, Liu X, Wu S, Wan B, Xu L, Li Y. Salvianolic acid B reverses multidrug resistance in nude mice bearing human colon cancer stem cells. *Mol Med Rep*. 2018;18(2):1323–1334. doi:10.3892/mmr.2018.9086.
  21. Shin SC, Kim S-H, You H, Kim B, Kim AC, Lee K-A, Yoon J-H, Ryu J-H, Lee W-J. *Drosophila* microbiome modulates host developmental and metabolic homeostasis via insulin signaling. *Science*. 2011;334(6056):670–674. doi:10.1126/science.1212782.
  22. Wang X, Yang Y, Huycke MM. Commensal bacteria drive endogenous transformation and tumour stem cell marker expression through a bystander effect. *Gut*. 2015;64(3):459–468. doi:10.1136/gutjnl-2014-307213.
  23. Sahu U, Choudhury A, Parvez S, Biswas S, Kar S. Induction of intestinal stemness and tumorigenicity by aberrant internalization of commensal non-pathogenic *E. coli*. *Cell Death Dis*. 2017;8(3):e2667. doi:10.1038/cddis.2017.27.
  24. Ko SH, Rhoda J, Jeon JI, Kim Y-J, Woo HA, Lee YK, Kim JM. *Bacteroides fragilis* Enterotoxin Upregulates Heme Oxygenase-1 in Intestinal Epithelial Cells via a Mitogen-Activated Protein Kinase- and NF- $\kappa$ B-Dependent Pathway, Leading to Modulation of Apoptosis. *Infect Immun*. 2016;84(9):2541–2554. doi:10.1128/IAI.00191-16.
  25. Geis AL, Fan H, Wu X, Wu S, Huso DL, Wolfe JL, Sears CL, Pardoll DM, Housseau F. Regulatory T-cell Response to Enterotoxigenic *Bacteroides fragilis* Colonization Triggers IL17-Dependent Colon Carcinogenesis. *Cancer Discov*. 2015;5(10):1098–1109. doi:10.1158/2159-8290.CD-15-0447.
  26. Thiele Orberg E, Fan H, Tam AJ, Dejea CM, Destefano Shields CE, Wu S, Chung L, Finard BB, Wu X, Fathi P, et al. The myeloid immune signature of enterotoxigenic *Bacteroides fragilis*-induced murine colon tumorigenesis. *Mucosal Immunol*. 2017;10(2):421–433. doi:10.1038/mi.2016.53.
  27. Kanehisa M, Goto S, Sato Y, Kawashima M, Furumichi M, Tanabe M. Data, information, knowledge and principle: back to metabolism in KEGG. *Nucleic Acids Res*. 2014;42(Database issue):D199–205. doi:10.1093/nar/gkt1076.
  28. Kaufhold S, Garbán H, Bonavida B. Yin Yang 1 is associated with cancer stem cell transcription factors (SOX2, OCT4, BMI1) and clinical implication. *J Exp Clin Cancer Res*. 2016;35:84. doi:10.1186/s13046-016-0359-2.
  29. Boyer LA, Lee TI, Cole MF, Johnstone SE, Levine SS, Zucker JP, Guenther MG, Kumar RM, Murray HL, Jenner RG, et al. Core transcriptional regulatory circuitry in human embryonic stem cells. *Cell*. 2005;122(6):947–956. doi:10.1016/j.cell.2005.08.020.
  30. Zhang J, Espinoza LA, Kinders RJ, Lawrence SM, Pfister TD, Zhou M, Veenstra TD, Thorgeirsson SS, Jessup JM. NANOG modulates stemness in human colorectal cancer. *Oncogene*. 2013;32(37):4397–4405. doi:10.1038/onc.2012.461.
  31. Yifang H, Smyth GK. ELDA: extreme limiting dilution analysis for comparing depleted and enriched populations in stem cell and other assays. *J Immunol Methods*. 2009;347(1–2):70–78. doi:10.1016/j.jim.2009.06.008.
  32. Krautkramer KA, Kreznar JH, Romano KA, Vivas EI, Barrett-Wilt GA, Rabaglia ME, Keller MP, Attie AD, Rey FE, Denu JM. Diet-microbiota interactions mediate global epigenetic programming in multiple host tissues. *Mol Cell*. 2016;64(5):982–992. doi:10.1016/j.molcel.2016.10.025.
  33. Chen J, Liu H, Liu J, Qi J, Wei B, Yang J, Liang H, Chen Y, Chen J, Wu Y, et al. H3K9 methylation is a barrier during somatic cell reprogramming into iPSCs. *Nat Genet*. 2013;45(1):34–42. doi:10.1038/ng.2491.
  34. Kim T-D, Jin F, Shin S, Oh S, Lightfoot SA, Grande JP, Johnson AJ, van Deursen JM, Wren JD, Janknecht R, et al. Histone demethylase JMJD2A drives prostate tumorigenesis through transcription factor ETV1. *J Clin Invest*. 2016;126(2):706–720. doi:10.1172/JCI78132.
  35. Young LC, McDonald DW, Hendzel MJ. Kdm4b histone demethylase is a DNA damage response protein and confers a survival advantage following gamma-irradiation. *J Biol Chem*. 2013;288(29):21376–21388. doi:10.1074/jbc.M113.491514.
  36. Buxadé M, Lunazzi G, Minguión J, Iborra S, Berga-Bolaños R, Del Val M, Aramburu J, López-Rodríguez C. Gene expression induced by Toll-like receptors in macrophages requires the transcription factor NFAT5. *J Exp Med*. 2012;209(2):379–393. doi:10.1084/jem.20111569.
  37. Stappers MH, Janssen NA, Oosting M, Plantinga TS, Arvis P, Mouton JW, Joosten LAB, Netea MG, Gyssens IC. A role for TLR1, TLR2 and NOD2 in cytokine induction by *Bacteroides fragilis*. *Cytokine*. 2012;60(3):861–869. doi:10.1016/j.cyto.2012.08.019.
  38. Lukiw WJ. *Bacteroides fragilis* Lipopolysaccharide and Inflammatory Signaling in Alzheimer's Disease. *Front Microbiol*. 2016;7:1544. doi:10.3389/fmicb.2016.01544.
  39. Brennan CA, Garrett WS. Gut Microbiota, Inflammation, and Colorectal Cancer. *Annu Rev Microbiol*. 2016;70:395–411. doi:10.1146/annurev-micro-102215-095513.
  40. Martins MD, Jiao Y, Larsson L, Almeida LO, Garaicoa-Pazmino C, Le JM, Squarize CH, Inohara N, Giannobile WV, Castilho RM. Epigenetic Modifications of Histones in Periodontal Disease. *J Dent Res*. 2016;95(2):215–222. doi:10.1177/0022034515611876.

41. Allen J, Hao S, Sears CL, Timp W. Epigenetic changes induced by *Bacteroides fragilis* toxin. *Infect Immun*. 2019;87(6):pii: e00447-18.
42. Novo CL, Tang C, Ahmed K, Djuric U, Fussner E, Mullin NP, Morgan NP, Hayre J, Sienerth AR, Elderkin S, et al. The pluripotency factor Nanog regulates pericentromeric heterochromatin organization in mouse embryonic stem cells. *Genes Dev*. 2016;30(9):1101–1115. doi:10.1101/gad.275685.115.
43. Meshorer E, Misteli T. Chromatin in pluripotent embryonic stem cells and differentiation. *Nat Rev Mol Cell Biol*. 2006;7(7):540–546. doi:10.1038/nrm1938.
44. Kooistra SM, Helin K. Molecular mechanisms and potential functions of histone demethylases. *Nat Rev Mol Cell Biol*. 2012;13(5):297–311. doi:10.1038/nrm3327.
45. Fu L, Chen L, Yang J, Ye T, Chen Y, Fang J. HIF-1 $\alpha$ -induced histone demethylase JMJD2B contributes to the malignant phenotype of colorectal cancer cells via an epigenetic mechanism. *Carcinogenesis*. 2012;33(9):1664–1673. doi:10.1093/carcin/bgs217.
46. Chen L, Fu L, Kong X, Xu J, Wang Z, Ma X, Akiyama Y, Chen Y, Fang J. Jumonji domain-containing protein 2B silencing induces DNA damage response via STAT3 pathway in colorectal cancer. *Br J Cancer*. 2014;110(4):1014–1026. doi:10.1038/bjc.2013.808.
47. Fu L-N, Wang Y-Q, Tan J, Xu J, Gao Q-Y, Chen Y-X, Fang J-Y. Role of JMJD2B in colon cancer cell survival under glucose-deprived conditions and the underlying mechanisms. *Oncogene*. 2018;37(3):389–402. doi:10.1038/onc.2017.345.
48. Das PP, Shao Z, Beyaz S, Apostolou E, Pinello L, De Los Angeles A, O'Brien K, Atsma J, Fujiwara Y, Nguyen M. Distinct and Combinatorial Functions of Jmjd2b/Kdm4b and Jmjd2c/Kdm4c in Mouse Embryonic Stem Cell Identity. *Mol Cell*. 2014;53(1):32–48. doi:10.1016/j.molcel.2013.11.011.
49. Pedersen MT, Kooistra SM, Radziszewska A, Laugesen A, Johansen JV, Hayward DG, Nilsson J, Agger K, Helin K. Continual removal of H3K9 promoter methylation by Jmjd2 demethylases is vital for ESC self-renewal and early development. *Embo J*. 2016;35(14):1550–1564. doi:10.15252/embj.201593317.
50. Lee SD, Choi SY, Lim SW, Lamitina ST, Ho SN, Go WY, Kwon HM. TonEBP stimulates multiple cellular pathways for adaptation to hypertonic stress: organic osmolyte-dependent and -independent pathways. *Am J Physiol Renal Physiol*. 2011;300(3):F707–15. doi:10.1152/ajprenal.00227.2010.
51. Neuhofer W, Beck FX. Cell survival in the hostile environment of the renal medulla. *Annu Rev Physiol*. 2005;67:531–555. doi:10.1146/annurev.physiol.67.031103.154456.
52. Christoph K, Beck FX, Neuhofer W. Osmoadaptation of Mammalian cells—an orchestrated network of protective genes. *Curr Genomics*. 2007;8(4):209–218. doi:10.2174/138920207781386979.
53. López-Rodríguez C, Antos CL, Shelton JM, Richardson JA, Lin F, Novobrantseva TI, Bronson RT, Igarashi P, Rao A, Olson EN. Loss of NFAT5 results in renal atrophy and lack of tonicity-responsive gene expression. *Proc Natl Acad Sci U S A*. 2004;101(8):2392–2397. doi:10.1073/pnas.0308703100.
54. Trama J, Lu Q, Hawley RG, Ho SN. The NFAT-related protein NFATL1 (TonEBP/NFAT5) is induced upon T cell activation in a calcineurin-dependent manner. *J Immunol*. 2000;165(9):4884–4894. doi:10.4049/jimmunol.165.9.4884.
55. Erridge C, Pridmore A, Eley A, Stewart J, Poxton IR. Lipopolysaccharides of *Bacteroides fragilis*, *Chlamydia trachomatis* and *Pseudomonas aeruginosa* signal via toll-like receptor 2. *J Med Microbiol*. 2004;53(Pt 8):735–740. doi:10.1099/jmm.0.45598-0.
56. Alhawi M, Stewart J, Erridge C, Patrick S, Poxton IR. *Bacteroides fragilis* signals through Toll-like receptor (TLR) 2 and not through TLR4. *J Med Microbiol*. 2009;58(Pt 8):1015–1022. doi:10.1099/jmm.0.009936-0.
57. Ahmadi Badi S, Khatami SH, Irani SH, Siadat SD. Induction effects of *bacteroides fragilis* derived outer membrane vesicles on toll like receptor 2, toll like receptor 4 genes expression and cytokines concentration in human intestinal epithelial cells. *Cell J*. 2019;21(1):57–61. doi:10.22074/cellj.2019.5750.
58. Tzianabos AO, Onderdonk AB, Rosner B, Cisneros RL, Kasper DL. Structural features of polysaccharides that induce intra-abdominal abscesses. *Science*. 1993;262(5132):416–419. doi:10.1126/science.8211161.
59. Krinos CM, Coyne MJ, Weinacht KG, Tzianabos AO, Kasper DL, Comstock LE. Extensive surface diversity of a commensal microorganism by multiple DNA inversions. *Nature*. 2001;414(6863):555–558. doi:10.1038/35107092.
60. Mancuso G, Midiri A, Biondo C, Beninati C, Gambuzza M, Macrì D, Bellantoni A, Weintraub A, Espevik T, Teti G, et al. *Bacteroides fragilis*-derived lipopolysaccharide produces cell activation and lethal toxicity via toll-like receptor 4. *Infect Immun*. 2005;73(9):5620–5627. doi:10.1128/IAI.73.9.5620-5627.2005.
61. Zhou J, Huang XY, Ren LC, Tang Y. The influence of the LPS from *Bacteroides fragilis* on the secretion of IL-2 and IL-4 from the peripheral blood mononuclear cells of normal volunteers. *Zhonghua Shao Shang Za Zhi*. 2003;19:82–85.
62. Gorreja F, Rush ST, Kasper DL, Meng D, Walker WA. The developmentally regulated fetal enterocyte gene, ZP4, mediates anti-inflammation by the symbiotic bacterial surface factor polysaccharide A on *Bacteroides fragilis*. *Am J Physiol Gastrointest Liver Physiol*. 2019;317(4):G398–G407. doi:10.1152/ajpgi.00046.2019.
63. Sears CL, Geis AL, Housseau F. *Bacteroides Fragilis* subverts mucosal biology: from symbiont to colon carcinogenesis. *J Clin Invest*. 2014;124(10):4166–4172. doi:10.1172/JCI72334.

64. Allen J, Stephanie Hao CL, Sears W. Timp Epigenetic Changes Induced by *Bacteroides fragilis* Toxin. *Infect Immun*. 2019;87(6):e00447–18. doi:10.1128/IAI.00447-18.
65. Rhee K-J, Wu S, Wu X, Huso DL, Karim B, Franco AA, Rabizadeh S, Golub JE, Mathews LE, Shin J, et al. Induction of persistent colitis by a human commensal, enterotoxigenic *Bacteroides fragilis*, in wild-type C57BL/6 mice. *Infect Immun*. 2009;77(4):1708–1718. doi:10.1128/IAI.00814-08.
66. Johnson S, Chen H, Lo PK. *In vitro* tumorsphere formation assays. *Bio Protoc*. 2013;3(3):pii: e325. doi:10.21769/BioProtoc.325.
67. Livak KJ, Schmittgen TD. Analysis of relative gene expression data using real-time quantitative PCR and the 2<sup>(-Delta Delta C(T))</sup> Method. *Methods*. 2001;25(4):402–408. doi:10.1006/meth.2001.1262.
68. Xue X, Shah YM. *In vitro* organoid culture of primary mouse colon tumors. *J Vis Exp*. 2013;75:e50210.